

# MBM-Aided Uplink Cooperative NOMA With Hardware Impairments and Imperfect CSI

Mehmet Can<sup>1</sup>, Graduate Student Member, IEEE, Ibrahim Altunbas<sup>2</sup>, Senior Member, IEEE, and Ertugrul Basar<sup>2</sup>, Senior Member, IEEE

**Abstract**—In this letter, we propose a media-based modulation (MBM)-aided uplink cooperative non-orthogonal multiple access (NOMA) scheme operating under hardware impairments and imperfect channel state information (CSI). In this scheme, the signal of the far user is transmitted with conventional modulation via the best pattern created from the ON/OFF status of the radio frequency (RF) mirrors. The near user decodes the far user's signal and transmits with the MBM technique by superposing its information. The bit error rate (BER) expressions of the proposed system for both users are derived under hardware impairments and imperfect CSI. Simulation results validate the derived BER expressions. Moreover, the proposed system is compared with systems in which the spatial modulation (SM) aided NOMA, generalized SM aided NOMA, and conventional NOMA applied at the near user. It has been shown that the proposed system is more robust to hardware impairments and imperfect CSI and outperforms these systems.

**Index Terms**—Media-based modulation (MBM), non-orthogonal multiple access (NOMA), hardware impairments, channel estimation errors, cooperative relaying, bit error rate (BER).

## I. INTRODUCTION

NON-ORTHOGONAL multiple access (NOMA) is an emerging technique for satisfying the requirements of next-generation wireless communication, which are mainly the efficient use of frequency bands and high spectral efficiency. The basic idea of NOMA is to serve multiple users in the same radio resources by allowing some level of interference. Typically, the successive interference cancellation (SIC) technique is used at the receiver. In recent years, NOMA has been widely discussed in several aspects. In [1], outage probability and ergodic sum-rate of the NOMA is investigated. The pairwise error probability (PEP) and the bit error rate (BER) of NOMA are studied in [2]. Moreover, NOMA is introduced for cooperative networks, and results show that cooperative NOMA provides better outage performance than orthogonal multiple access and conventional NOMA [3].

Index modulation (IM) is another spectral and energy efficient technique that allows the transmission of information with the main components of the digital communication system [4]. Spatial modulation (SM) [5] and space shift keying

(SSK) [6] are the two most known IM techniques in which antenna indices are used for information transfer.

Media-based modulation (MBM) is another IM technique that can provide high spectral efficiency using a single radio frequency (RF) chain, the same as in SM and SSK [7]. In MBM, the transmit antenna is equipped with RF mirrors or electronic switches. Information bits are used to set the ON/OFF status of RF mirrors, and switching between the ON/OFF status enables unique mirror activation patterns (MAPs). While SM and SSK need exponential increase in the number of the transmit antennas to increase the spectral efficiency, MBM can achieve the same spectral efficiency by linearly increasing the number of RF mirrors even using a single transmit antenna. A combination of NOMA and IM schemes are also considered in the literature. In particular, SM-aided NOMA is proposed and investigated for the vehicle-to-vehicle system in [8]. NOMA is combined with generalized SSK that superposition signal is transmitted using multiple active transmit antennas in [9]. A cooperative relaying system using SM-aided NOMA is introduced in [10]. Precoded SM and NOMA are integrated to exploit their benefits for supporting high-rate downlink communication in [11]. A NOMA-based relaying system, where MBM is applied at the source to improve error performance at the relay, is proposed in [12].

The studies mentioned above assume ideal hardware and perfect channel state information (CSI). In practical scenarios, however, the hardware suffers from phase noise and I/Q imbalance [13], and CSI can be imperfect due to the channel estimation errors. The impact of hardware impairments at the transmitter and receiver sides on SSK is investigated in [14]. The effects of the channel estimation errors on the performance of SM are discussed in [15]. Moreover, the joint impact of hardware and channel imperfections on SM systems is presented in [16].

In this letter, we propose an MBM-aided uplink cooperative NOMA scheme considering two users. In this scheme, both users are equipped with a single antenna and multiple RF mirrors. MAP selection is applied at the far user, and the signal is transmitted by using conventional modulation. The near user acts as the cooperative node and detects the far user's signal. The superposition signal, which is the combination of the far user's decoded signal and a part of the near user's information, is transmitted via the MBM technique. The BER expressions of the users are derived under nonideal hardware and imperfect CSI. Simulation results validate the theoretical analysis. Moreover, the proposed system is compared with the systems that conventional, SM-aided, and GSM-aided NOMA are applied at the near user. Our results show that the proposed system outperforms these systems in terms of BER

Manuscript received January 8, 2021; revised February 14, 2021; accepted March 1, 2021. Date of publication March 2, 2021; date of current version June 10, 2021. This work was supported by the Scientific and Technological Research Council of Turkey (TUBITAK) under Grant no. 117E869. The associate editor coordinating the review of this letter and approving it for publication was Y. Xiao. (Corresponding author: Mehmet Can.)

Mehmet Can and Ibrahim Altunbas are with the Faculty of Electrical and Electronics Engineering, Istanbul Technical University, 34469 Istanbul, Turkey (e-mail: canmehmet@itu.edu.tr; ibraltunbas@itu.edu.tr).

Ertugrul Basar is with the Communications Research and Innovation Laboratory (CoreLab), Department of Electrical and Electronics Engineering, Koç University, 34450 Istanbul, Turkey (e-mail: ebasar@ku.edu.tr).

Digital Object Identifier 10.1109/LCOMM.2021.3063459

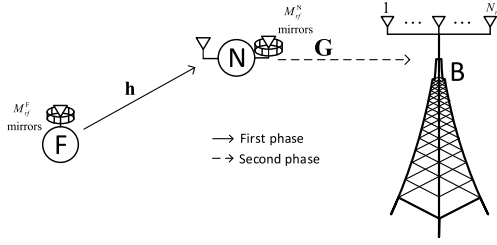


Fig. 1. System model of the MBM-aided uplink cooperative NOMA.

performance and is more robust to hardware impairments and imperfect CSI.<sup>1</sup>

## II. SYSTEM MODEL

The system model of the proposed MBM-aided uplink cooperative NOMA scheme is given in Fig. 1. In this scheme, far (F) and near (N) users are equipped with a single transmit antenna with  $M_{rf}^F$  and  $M_{rf}^N$  RF mirrors, respectively. Therefore,  $N_{rf}^F = 2^{M_{rf}^F}$  and  $N_{rf}^N = 2^{M_{rf}^N}$  MAPs are possible for F and N, respectively. In transmission, only a single MAP can be activated, and the PSK signal is transmitted via the activated MAP. N and the base station (B) are equipped with single and  $N_r$  receive antennas, respectively. We assume that the direct link between F and B are not available. N can directly communicate with B, and F communicates with B via N. All nodes are operated in half-duplex mode, so the overall transmission consists of two phases.

We assume flat fading channels. The channel coefficients vector from F to N is denoted as  $\mathbf{h} \in \mathbb{C}^{N_{rf}^F \times 1}$ , and  $h_i$  defines the complex channel coefficient corresponding to the  $i$ th MAP ( $i = 1, 2, \dots, N_{rf}^F$ ). The channel coefficients matrix from N to B is denoted as  $\mathbf{G} \in \mathbb{C}^{N_{rf}^N \times N_r}$ , and  $g_{k,r}$  defines the complex channel coefficient corresponding to the  $k$ th MAP and  $r$ th receive antenna ( $k = 1, 2, \dots, N_{rf}^N$ ,  $r = 1, 2, \dots, N_r$ ). The elements of  $\mathbf{h}$  and  $\mathbf{G}$  are considered to be independent and identically distributed (i.i.d.) random variables and follow  $\mathcal{CN}(0, \sigma_h^2)$  and  $\mathcal{CN}(0, \sigma_g^2)$ , respectively. This means that the envelope of the channel coefficients follow Rayleigh distribution. The channels are estimated with the least squares (LS) method as  $\hat{h}_i$  and  $\hat{g}_{k,r}$  instead of  $h_i$  and  $g_{k,r}$ , respectively. The channel estimation errors are modeled as  $e_h = \hat{h}_i - h_i$  and  $e_g = \hat{g}_{k,r} - g_{k,r}$ , which are distributed as  $\mathcal{CN}(0, \sigma_{e,h}^2)$  and  $\mathcal{CN}(0, \sigma_{e,g}^2)$ , respectively [15]. Consequently, the erroneously estimated channel coefficients  $\hat{h}_i$  and  $\hat{g}_{k,r}$  follow  $\mathcal{CN}(0, \sigma_h^2 + \sigma_{e,h}^2)$  and  $\mathcal{CN}(0, \sigma_g^2 + \sigma_{e,g}^2)$ , respectively.

Since the performance of the MBM technique may not be satisfactory for a small number of receive antennas [17] and N has a single receive antenna, we propose the MAP selection technique, which has the same principle as the transmit antenna selection [18], [19]. The MAP selection is

<sup>1</sup>Notation: Bold capital and bold lowercase letters denote matrices and vectors, respectively.  $|\cdot|$  and  $(\cdot)$  denote the absolute value and the binomial coefficient, respectively.  $P(\cdot)$  stands for the probability of an event.  $\mathbb{E}[X]$ ,  $f_X(x)$ , and  $\mathcal{M}_X(s)$  denote the mean, probability density function (PDF), and moment generating function (MGF) of a random variable  $X$ .  $\mathcal{CN}(\mu, \sigma^2)$  denotes complex normal distribution with mean  $\mu$  and variance  $\sigma^2$ .  $\Gamma(\alpha, \beta)$  denotes gamma distribution with shape parameter  $\alpha$  and scale parameter  $\beta$ .  $Q(\cdot)$  denotes the Gaussian-Q function.

applied at F, and the selected MAP index at F is determined by

$$i_* = \arg \max_i |\hat{h}_i|, \quad i = 1, \dots, N_{rf}^F. \quad (1)$$

The  $M_F$ -PSK signal of F is transmitted via the selected MAP. Thus,  $\mathcal{S}_F = \log_2 M_F$  bits can be transmitted from F during a transmission interval. In the first phase, the received signal at N is expressed as

$$y^{\text{FN}} = \sqrt{P_F} h_{i_*} (x_l + \eta_t^F) + \eta_r^N + n^N \quad (2)$$

where  $P_F$  is the transmitter power at F,  $x_l$  is the corresponding  $M_F$ -PSK signal, and  $n^N$  is the additive noise at N and follows  $\mathcal{CN}(0, N_0)$  where  $N_0$  is one-sided power spectral density of the additive white Gaussian noise (AWGN). The parameters  $\eta_t^F$  and  $\eta_r^N$  are independent distortion noises from impairments in the transmitter of F and receiver of N, respectively. They are modeled as  $\eta_t^F \sim \mathcal{CN}(0, \kappa_{t,F}^2 P_F)$  and  $\eta_r^N \sim \mathcal{CN}(0, \kappa_{r,N}^2 P_F |h_{i_*}|^2)$ , respectively, where  $\kappa_{t,F}$  and  $\kappa_{r,N}$  are the distortion level of the impairments in the transmitter of F and receiver of N, respectively. The overall impact of the impairments in both F and N can be characterized by [13]

$$\kappa_{\text{FN}} = \sqrt{\kappa_{t,F}^2 + \kappa_{r,N}^2}. \quad (3)$$

By using (3), we can rewrite (2) as

$$y^{\text{FN}} = \sqrt{P_F} h_{i_*} x_l + \chi^N \quad (4)$$

where  $\chi^N = \sqrt{P_F} h_{i_*} \eta_t^F + \eta_r^N + n^N$  and follows  $\mathcal{CN}(0, \kappa_{\text{FN}}^2 P_F |h_{i_*}|^2 + N_0)$ .

The signal transmitted from F is detected at N as

$$\hat{x}_l = \arg \min_l |y^{\text{FN}} - \sqrt{P_F} \hat{h}_{i_*} x_l|^2 \quad (5)$$

by using the maximum-likelihood (ML) detector.

In the second phase, MBM-aided NOMA is applied at N. The bits of N split into two parts: the first  $M_{rf}^N$  bits are used for the control of the ON/OFF status of RF mirrors and mapped into the  $k$ th MAP, and the remaining bits are mapped to  $M_N$ -PSK signal  $x_q$ . Thus,  $\mathcal{S}_N = M_{rf}^N + \log_2 M_N$  bits can be transmitted for N during a transmission interval. In transmission, the  $k$ th MAP is activated to transmit the superposition signal of F and N based on NOMA. The received signal at the  $r$ th receive antenna of B is expressed as

$$y_r^{\text{NB}} = \sqrt{P_N} g_{k,r} (s_{lq} + \eta_t^N) + \eta_r^B + n_r^B \quad (6)$$

where  $P_N$  is the transmitter power at N, and  $n_r^B$  is the additive noise at B and follows  $\mathcal{CN}(0, N_0)$ .  $s_{lq}$  is the superposition signal, which is expressed as  $s_{lq} = \sqrt{\alpha_F} \hat{x}_l + \sqrt{\alpha_N} x_q$ , where  $\alpha_F$  and  $\alpha_N$  are the power allocation coefficient for F and N, respectively, with  $\alpha_F + \alpha_N = 1$ . The parameters  $\eta_t^N$  and  $\eta_r^B$  are independent distortion noises from impairments in the transmitter of N and receiver of B, respectively. They are modeled as  $\eta_t^N \sim \mathcal{CN}(0, \kappa_{t,N}^2 P_N)$  and  $\eta_r^B \sim \mathcal{CN}(0, \kappa_{r,B}^2 P_N |g_{k,r}|^2)$ , respectively, where  $\kappa_{t,N}$  and  $\kappa_{r,B}$  are the distortion level of the impairments in the transmitter of N and receiver of B, respectively. As in (3), the aggregation level of hardware

impairments at both N and B can be characterized by  $\kappa_{\text{NB}} = \sqrt{\kappa_{t,\text{N}}^2 + \kappa_{r,\text{B}}^2}$ , and (6) can be simplified as

$$y_r^{\text{NB}} = \sqrt{P_{\text{N}}}g_{k,r}s_{lq} + \chi^{\text{B}} \quad (7)$$

where  $\chi^{\text{B}} = \sqrt{P_{\text{N}}}g_{k,r}\eta_t^{\text{N}} + \eta_r^{\text{B}} + n_r^{\text{B}}$  and follows  $\mathcal{CN}(0, \kappa_{\text{NB}}^2 P_{\text{N}}|g_{k,r}|^2 + N_0)$ .

At B, the signals of the users can be detected by using SIC or joint ML detector. Because the joint ML detector achieves optimal performance in terms of BER for uplink systems compared to the SIC technique [20], B jointly estimates the MAP index  $\hat{k}$  and the signal  $\hat{s}_{lq}$  with the joint ML rule, which is expressed as

$$[\hat{k}, \hat{s}_{lq}] = \arg \min_{k,l,q} \sum_{r=1}^{N_r} |y_r^{\text{NB}} - \sqrt{P_{\text{N}}}\hat{g}_{k,r}s_{lq}|^2. \quad (8)$$

### III. PERFORMANCE ANALYSIS

In this section, we analyze the performance of the proposed system in terms of BER. We first investigate the near user's BER performance and then consider the BER for the far user.

#### A. BER for the Near User

The average BER for N can be evaluated by using the union bound method [21] as follows

$$P_{e,\text{N}} \leq \frac{1}{N_{r,f}^{\text{N}} M_{\text{F}} M_{\text{N}}} \sum_{k,s_{lq}} \sum_{\hat{k}, \hat{s}_{lq}} P([k, s_{lq}] \rightarrow [\hat{k}, \hat{s}_{lq}]) \frac{\xi_{kq, \hat{k}\hat{q}}}{\mathcal{S}_{\text{N}}} \quad (9)$$

where  $P([k, s_{lq}] \rightarrow [\hat{k}, \hat{s}_{lq}])$  is the PEP at B and stands for the erroneously detecting the superposition signal as  $\hat{s}_{lq}$  and MAP index as  $\hat{k}$  when the signal  $s_{lq}$  transmitted from the  $k$ th MAP.  $\xi_{kq, \hat{k}\hat{q}}$  denotes the number of bits in error between transmitted and received information of N.

We first derive the conditional PEP from (8) as

$$\begin{aligned} & P([k, s_{lq}] \rightarrow [\hat{k}, \hat{s}_{lq}] | \hat{\mathbf{G}}) \\ &= Q \left( \sqrt{\frac{P_{\text{N}} \sum_{r=1}^{N_r} |\hat{g}_{k,r}s_{lq} - \hat{g}_{\hat{k},r}\hat{s}_{lq}|^2}{2(N_0 + P_{\text{N}}\sigma_{e,g}^2|s_{lq}|^2 + P_{\text{N}}\kappa^{\text{NB}}|g_{k,r}|^2)}} \right) \\ &\equiv Q(\sqrt{\gamma_{\text{N}}}) \end{aligned} \quad (10)$$

where  $\hat{\mathbf{G}}$  is the estimated channel matrix, and  $\gamma_{\text{N}} = \frac{P_{\text{N}} \sum_{r=1}^{N_r} |\hat{g}_{k,r}s_{lq} - \hat{g}_{\hat{k},r}\hat{s}_{lq}|^2}{2(N_0 + P_{\text{N}}\sigma_{e,g}^2|s_{lq}|^2 + P_{\text{N}}\kappa^{\text{NB}}\sigma_g^2)}$  is the equivalent expression obtained by replacing  $|g_{k,r}|^2$  by  $\sigma_g^2$ , in the same manner as those in [14], [16].

For flat Rayleigh fading channels,  $\gamma_{\text{N}}$  follows  $\Gamma(N_r, \bar{\gamma}_{\text{N}})$  where  $\bar{\gamma}_{\text{N}} = \frac{P_{\text{N}}(\sigma_g^2 + \sigma_{e,g}^2)v}{2(N_0 + P_{\text{N}}\sigma_{e,g}^2|s_{lq}|^2 + P_{\text{N}}\kappa^{\text{NB}}\sigma_g^2)}$ . Here,

$$v = \begin{cases} |s_{lq} - \hat{s}_{lq}|^2 & \text{if } k = \hat{k} \\ |s_{lq}|^2 + |\hat{s}_{lq}|^2 & \text{if } k \neq \hat{k}. \end{cases} \quad (11)$$

Using the MGF approach [21], the unconditional PEP can be obtained as

$$P([k, s_{lq}] \rightarrow [\hat{k}, \hat{s}_{lq}]) = \frac{1}{\pi} \int_0^{\frac{\pi}{2}} \mathcal{M}_{\gamma_{\text{N}}} \left( \frac{1}{2 \sin^2 \theta} \right) d\theta \quad (12)$$

where  $\mathcal{M}_{\gamma_{\text{N}}}(s)$  is given by  $\mathcal{M}_{\gamma_{\text{N}}}(s) = \frac{1}{(1+s\bar{\gamma}_{\text{N}})^{N_r}}$  [21].

Substituting this MGF into (12) and using [21, Eq.5A.4b], the PEP can be computed as

$$P([k, s_{lq}] \rightarrow [\hat{k}, \hat{s}_{lq}]) = \mu^{N_r} \sum_{j=0}^{N_r-1} \binom{N_r-1+j}{j} (1-\mu)^j \quad (13)$$

where  $\mu = \frac{1}{2} \left( 1 - \sqrt{\frac{\bar{\gamma}_{\text{N}}/2}{1+\bar{\gamma}_{\text{N}}/2}} \right)$ . By substituting (13) into (9), the BER for N can be obtained.

#### B. BER for Far User

The BER of F depends on two conditions considering the signal of F is detected correctly or not in the first phase. Thus, the BER for F can be divided into two parts as [10]

$$P_{e,\text{F}} \approx (1 - P_{e,\text{F}_1})P_{c,\text{F}_2} + P_{e,\text{F}_1}P_{e,\text{F}_2} \quad (14)$$

where  $P_{e,\text{F}_1}$  is the BER for F at the first phase.  $P_{c,\text{F}_2}$  is the BER for F under the condition that F's signal is correctly detected in the first phase.  $P_{e,\text{F}_2}$  is the BER for F when the errors occur in the first phase.

$P_{e,\text{F}_1}$  can be evaluated as [22]

$$\begin{aligned} P_{e,\text{F}_1} &= \frac{2}{\log_2 M_{\text{F}}} \mathbb{E} \left[ Q \left( \sqrt{\frac{2P_{\text{F}}|\hat{h}_{i_*}|^2 \sin^2 \left( \frac{\pi}{M_{\text{F}}} \right)}{N_0 + P_{\text{F}}\sigma_{e,h}^2 + P_{\text{F}}\kappa^{\text{FN}}|h_{i_*}|^2}} \right) \right] \\ &\equiv \frac{2}{\log_2 M_{\text{F}}} \mathbb{E} \left[ Q \left( \sqrt{2\gamma_{\text{F}}} \sin \left( \frac{\pi}{M_{\text{F}}} \right) \right) \right] \end{aligned} \quad (15)$$

where  $\gamma_{\text{F}} = \frac{P_{\text{F}}|\hat{h}_{i_*}|^2}{N_0 + P_{\text{F}}\sigma_{e,h}^2 + P_{\text{F}}\kappa^{\text{FN}}\sigma_h^2}$  is the equivalent expression obtained by replacing  $|h_{i_*}|^2$  by  $\sigma_h^2$ .

Because the MAP selection is applied at F, the PDF of  $\gamma_{\text{F}}$  is given by

$$\begin{aligned} f_{\gamma_{\text{F}}}(x) &= N_{r,f}^{\text{F}} \frac{1}{\bar{\gamma}_{\text{F}}} e^{-\frac{x}{\bar{\gamma}_{\text{F}}}} (1 - e^{-\frac{x}{\bar{\gamma}_{\text{F}}}})^{N_{r,f}^{\text{F}}} \\ &= N_{r,f}^{\text{F}} \frac{1}{\bar{\gamma}_{\text{F}}} e^{-\frac{x}{\bar{\gamma}_{\text{F}}}} \sum_{m=0}^{N_{r,f}^{\text{F}}-1} \binom{N_{r,f}^{\text{F}}-1}{m} (-1)^m e^{-\frac{xm}{\bar{\gamma}_{\text{F}}}} \end{aligned} \quad (16)$$

where  $\bar{\gamma}_{\text{F}} = \frac{P_{\text{F}}(\sigma_h^2 + \sigma_{e,h}^2)}{N_0 + P_{\text{F}}\sigma_{e,h}^2 + P_{\text{F}}\kappa^{\text{FN}}\sigma_h^2}$ .

Using the MGF approach, (15) can be obtained as [22, Eq.6.75]

$$P_{e,\text{F}_1} = \frac{1}{\pi} \int_0^{\frac{(M_{\text{F}}-1)\pi}{M_{\text{F}}}} \mathcal{M}_{\gamma_{\text{F}}} \left( \frac{\sin^2(\pi/M_{\text{F}})}{\sin^2 \theta} \right) d\theta. \quad (17)$$

Here,  $\mathcal{M}_{\gamma_{\text{F}}}(s)$  can be calculated by using [23, Eq.3.381.4] as

$$\begin{aligned} \mathcal{M}_{\gamma_{\text{F}}}(s) &= \int_0^{\infty} e^{-sx} f_{\gamma_{\text{F}}}(x) dx \\ &= \sum_{u=0}^{N_{r,f}^{\text{F}}} \binom{N_{r,f}^{\text{F}}-1}{u} (-1)^u \frac{N_{r,f}^{\text{F}}}{s\bar{\gamma}_{\text{F}} + u + 1}. \end{aligned} \quad (18)$$



In the case of correct detection of F's information in the first phase,  $P_{c,F_2}$  can be given as

$$P_{c,F_2} \leq \frac{1}{N_{rf}^N M_F M_N} \sum_{k,s_{lq}} \sum_{\hat{k},\hat{s}_{lq}} P([k,s_{lq}] \rightarrow [\hat{k},\hat{s}_{lq}]) \frac{\xi_{l,\hat{l}}}{S_F} \quad (19)$$

where  $\xi_{l,\hat{l}}$  is the number of bits in error between transmitted and received information of F in the second phase, and  $P([k,s_{lq}] \rightarrow [\hat{k},\hat{s}_{lq}])$  can be calculated by using (13).

In the case of erroneous detection in the first phase,  $P_{e,F_2}$  can be approximated by  $P_{e,F_2} \approx \frac{n_{F_2}}{S_F}$ , where  $n_{F_2}$  is the average bits of the erroneous detection of the  $M_F$ -PSK signal and given by [10]

$$n_{F_2} = \frac{1}{M_F - 1} \sum_{t=1}^{S_F} t \binom{S_F}{t}. \quad (20)$$

#### IV. NUMERICAL RESULTS

In this section, the BER of the proposed system with hardware impairments and imperfect CSI is evaluated via Monte Carlo simulations, and the results are compared with the analytical results. For comparison purposes, the performance of ideal hardware and perfect CSI cases are also considered. Moreover, the proposed system is compared with the systems that SM-aided NOMA (SM-NOMA) [8], GSM-aided NOMA (GSM-NOMA),<sup>2</sup> and conventional NOMA (C-NOMA) [1] are applied at N. Unless otherwise stated, we assume  $M_{rf}^F = \log_2 N_r$ ,  $\sigma_h^2 = \sigma_g^2 = 1$ ,  $\sigma_{e,h}^2 = \sigma_{e,g}^2 = \sigma_e^2$ ,  $\kappa_{FN} = \kappa_{NB} = \kappa$ , and  $P_F = P_N = P = 1$ . The BER results are provided as a function of the signal-to-noise ratio (SNR), which is defined as  $\text{SNR} = P/N_0$ .

In Fig. 2, the BER performance of the proposed system is given in the presence of ideal hardware ( $\kappa = 0$ ) for  $\sigma_e^2 \in \{0, 0.005, 0.01\}$ ,  $N_r \in \{2, 4\}$ ,  $M_F = 2$ ,  $M_{rf}^N = 1$ , and  $M_N = 2$ . The power allocation coefficients are arbitrarily chosen as  $\alpha_F = 0.8$  and  $\alpha_N = 0.2$ . As seen from Fig. 2, the BER performances of the users degrade with increasing  $\sigma_e^2$ , and the system exhibits an error floor behavior, especially at high SNRs. Moreover, the error floor is shifted to lower BER values with increasing  $N_r$ . For example, for  $\sigma_e^2 = 0.01$ , the error floor for F is observed at a BER value of  $3 \times 10^{-4}$  and  $2 \times 10^{-7}$  approximately for  $N_r = 2$  and 4, respectively. In addition, the derived BER expressions from (9) and (14) are well-matched with the simulation results.

Fig. 3 investigates the BER performance of the proposed system with nonideal hardware and imperfect CSI, where  $\kappa \in \{0.07, 0.1, 0.15\}$ ,  $\sigma_e^2 = 0.005$ , and  $N_r = 4$  for  $M_F = 2$ ,  $M_{rf}^N = 1$ ,  $M_N = 2$ ,  $\alpha_F = 0.8$ , and  $\alpha_N = 0.2$ . Also, the BER performance of the ideal case ( $\kappa = 0$ ,  $\sigma_e^2 = 0$ ) is given for comparison purposes. As expected, the BER performance worsens with increasing  $\kappa$ . For example, at a BER value of  $10^{-4}$ , approximately 1, 3, and 14 dB SNR loss is observed for each user compared with the ideal case for  $\kappa = 0.07, 0.1$ , and 0.15, respectively. Again, theoretical and simulation results are in agreement.

<sup>2</sup>GSM-NOMA is an advanced version of the scheme of [9] in which information bits of N are also mapped to a PSK signal besides antenna indices.

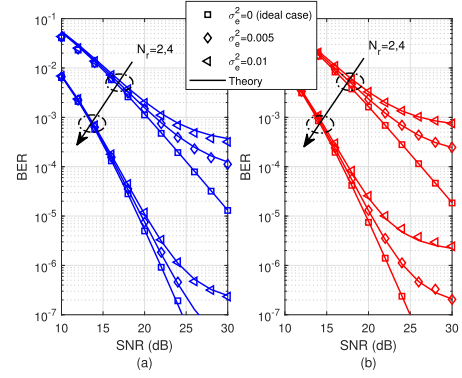


Fig. 2. BER performance of the proposed system with  $\kappa = 0$  and different values of  $\sigma_e^2 \in \{0, 0.005, 0.01\}$  (a) BER curves for F (b) BER curves for N.

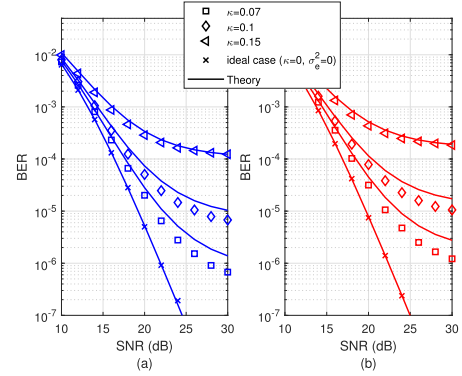


Fig. 3. BER performance of the proposed system with  $\sigma_e^2 = 0.005$  and different values of  $\kappa \in \{0.07, 0.1, 0.15\}$  (a) BER curves for F (b) BER curves for N.

In Fig. 4, the BER performance of the proposed system is compared with SM-NOMA, GSM-NOMA, and C-NOMA for  $[\mathcal{S}_F, \mathcal{S}_N] \in \{[2, 4], [3, 6]\}$  under ideal hardware and perfect CSI where  $N_r = 8$ . The power allocation coefficients are arbitrarily chosen as  $\alpha_F \in \{0.8, 0.9\}$  and  $\alpha_N \in \{0.2, 0.1\}$ , respectively.  $M_F$  is set as  $M_F \in \{4, 8\}$  for all systems. For the proposed system, the parameters are set as  $[M_{rf}^N, M_N] \in \{[3, 2], [5, 2]\}$ . The number of transmit antennas at N is chosen as 2, and  $M_N$  is set as  $M_N \in \{8, 32\}$  for SM-NOMA. The number of transmit antennas at N is chosen as 4, where 2 of them are active in the transmission, and  $M_N$  is set as  $M_N \in \{4, 16\}$  for GSM-NOMA. A single transmit antenna is considered at N, and  $M_N$  is set as  $M_N \in \{16, 64\}$  for C-NOMA. As seen from Fig. 4, at a BER value of  $10^{-5}$ , for F, the proposed system provides the same performance with GSM-NOMA and 2 dB SNR gain against SM-NOMA and C-NOMA for  $\mathcal{S}_F = 2$ . For  $\mathcal{S}_F = 3$ , the proposed system provides 8 dB SNR gain for F against SM-NOMA, GSM-NOMA, and C-NOMA. For N, at a BER value of  $10^{-5}$ , the proposed system provides 1, 4, and 10 dB SNR gains for  $\mathcal{S}_N = 4$ , and 9, 14, and 20 dB SNR gains for  $\mathcal{S}_N = 6$  compared to GSM-NOMA, SM-NOMA, and C-NOMA, respectively. The use of a lower-order PSK constellation has led to a superior performance for the proposed system compared to SM-NOMA, GSM-NOMA, and C-NOMA.

Finally, Fig. 5 compares the proposed system with SM-NOMA, GSM-NOMA, and C-NOMA under nonideal hardware and imperfect CSI where  $\kappa = 0.07$  and  $\sigma_e^2 = 0.005$  for  $\mathcal{S}_F = 2$  and  $\mathcal{S}_N = 4$  with the same parameters as

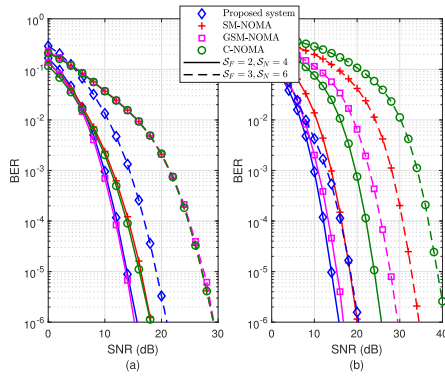


Fig. 4. BER performance comparison of the proposed system with SM-NOMA, GSM-NOMA and C-NOMA for ideal case ( $\kappa = 0$ ,  $\sigma_e^2 = 0$ ) (a) BER curves for F (b) BER curves for N.

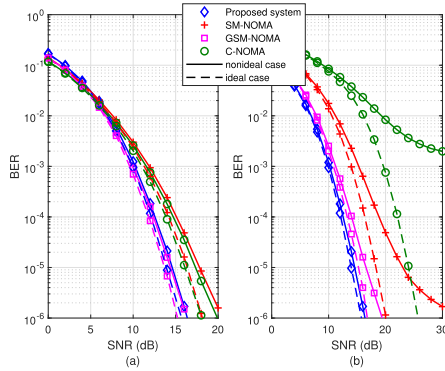


Fig. 5. BER performance comparison of the proposed system with SM-NOMA, GSM-NOMA, and C-NOMA for nonideal cases ( $\kappa = 0.07$ ,  $\sigma_e^2 = 0.005$ ) (a) BER curves for F (b) BER curves for N.

in Fig. 4. Also, the BER performance of the ideal case ( $\kappa = 0$ ,  $\sigma_e^2 = 0$ ) is given for comparison purposes. Because hardware impairments mostly affect the PSK signal, SM-NOMA, GSM-NOMA, and C-NOMA, which use higher-order PSK constellation, are more affected than MBM. Fig. 5 confirms that the proposed system is more robust to nonideal hardware and imperfect CSI compared to SM-NOMA, GSM-NOMA, and C-NOMA. In addition, the SNR gain of the proposed system compared to these systems is higher than the ideal case. At a BER value of  $10^{-5}$ , the proposed system provides the same performance with GSM-NOMA for F with 3 dB SNR gain against SM-NOMA and C-NOMA. For N, at a BER value of  $10^{-5}$ , the proposed system provides 2 and 10 dB SNR gains compared to GSM-NOMA and SM-NOMA, while C-NOMA is in error floor at the BER value of  $10^{-3}$ .

## V. CONCLUSION

In this letter, a novel MBM-aided cooperative uplink NOMA scheme is proposed. In this scheme, at the far user, the MAP selection is applied, and the signal of the far user is transmitted with conventional modulation. Information bits of the near user is split into two parts: the first part is used for the control of the ON/OFF status of the RF mirrors and the remaining part is mapped to conventional modulation signal and superposed with the decoded signal of the far user. The BER expressions of the users are derived, in the presence of nonideal hardware and imperfect CSI. It has been shown that

the proposed system outperforms SM-NOMA, GSM-NOMA, and C-NOMA schemes and more robust to nonideal hardware and imperfect CSI. Moreover, an extended version of the proposed system considering the multi-antenna and general multiuser case can be investigated as future work.

## REFERENCES

- [1] Z. Ding, Z. Yang, P. Fan, and H. V. Poor, "On the performance of non-orthogonal multiple access in 5G systems with randomly deployed users," *IEEE Signal Process. Lett.*, vol. 21, no. 12, pp. 1501–1505, Dec. 2014.
- [2] L. Bariah, S. Muhaidat, and A. Al-Dweik, "Error probability analysis of non-orthogonal multiple access over Nakagami- $m$  fading channels," *IEEE Trans. Commun.*, vol. 67, no. 2, pp. 1586–1599, Feb. 2019.
- [3] Z. Ding, M. Peng, and H. V. Poor, "Cooperative non-orthogonal multiple access in 5G systems," *IEEE Commun. Lett.*, vol. 19, no. 8, pp. 1462–1465, Aug. 2015.
- [4] E. Basar, "Index modulation techniques for 5G wireless networks," *IEEE Commun. Mag.*, vol. 54, no. 7, pp. 168–175, Jul. 2016.
- [5] R. Y. Mesleh, H. Haas, S. Sinanovic, C. W. Ahn, and S. Yun, "Spatial modulation," *IEEE Trans. Veh. Technol.*, vol. 57, no. 4, pp. 2228–2241, Jul. 2008.
- [6] J. Jeganathan, A. Ghrayeb, L. Szczecinski, and A. Ceron, "Space shift keying modulation for MIMO channels," *IEEE Trans. Wireless Commun.*, vol. 8, no. 7, pp. 3692–3703, Jul. 2009.
- [7] A. K. Khandani, "Media-based modulation: A new approach to wireless transmission," in *Proc. IEEE Int. Symp. Inf. Theory*, Jul. 2013, pp. 3050–3054.
- [8] Y. Chen, L. Wang, Y. Ai, B. Jiao, and L. Hanzo, "Performance analysis of NOMA-SM in vehicle-to-vehicle massive MIMO channels," *IEEE J. Sel. Areas Commun.*, vol. 35, no. 12, pp. 2653–2666, Dec. 2017.
- [9] J. W. Kim, S. Y. Shin, and V. C. M. Leung, "Performance enhancement of downlink NOMA by combination with GSSK," *IEEE Wireless Commun. Lett.*, vol. 7, no. 5, pp. 860–863, Oct. 2018.
- [10] Q. Li, M. Wen, E. Basar, H. V. Poor, and F. Chen, "Spatial modulation-aided cooperative NOMA: Performance analysis and comparative study," *IEEE J. Sel. Topics Signal Process.*, vol. 13, no. 3, pp. 715–728, Jun. 2019.
- [11] P. Yang, Y. Xiao, M. Xiao, and Z. Ma, "NOMA-aided precoded spatial modulation for downlink MIMO transmissions," *IEEE J. Sel. Topics Signal Process.*, vol. 13, no. 3, pp. 729–738, Jun. 2019.
- [12] M. Can, I. Altunbaş, and E. Basar, "NOMA-based downlink relaying with media-based modulation," *Phys. Commun.*, vol. 41, Aug. 2020, Art. no. 101116.
- [13] E. Bjornson, M. Matthaiou, and M. Debbah, "A new look at dual-hop relaying: Performance limits with hardware impairments," *IEEE Trans. Commun.*, vol. 61, no. 11, pp. 4512–4525, Nov. 2013.
- [14] A. Afana and S. Ikki, "Analytical framework for space shift keying MIMO systems with hardware impairments and co-channel interference," *IEEE Commun. Lett.*, vol. 21, no. 3, pp. 488–491, Mar. 2017.
- [15] E. Basar, U. Ayyolu, E. Panayirci, and H. V. Poor, "Performance of spatial modulation in the presence of channel estimation errors," *IEEE Commun. Lett.*, vol. 16, no. 2, pp. 176–179, Feb. 2012.
- [16] A. Afana, N. Abu-Ali, and S. Ikki, "On the joint impact of hardware and channel imperfections on cognitive spatial modulation MIMO systems: Cramer-Rao bound approach," *IEEE Syst. J.*, vol. 13, no. 2, pp. 1250–1261, Jun. 2019.
- [17] E. Basar, "Media-based modulation for future wireless systems: A tutorial," *IEEE Wireless Commun.*, vol. 26, no. 5, pp. 160–166, Oct. 2019.
- [18] Z. Chen, J. Yuan, and B. Vucetic, "Analysis of transmit antenna selection/maximal-ratio combining in Rayleigh fading channels," *IEEE Trans. Veh. Technol.*, vol. 54, no. 4, pp. 1312–1321, Jul. 2005.
- [19] Y. Naresh and A. Chockalingam, "On media-based modulation using RF mirrors," *IEEE Trans. Veh. Technol.*, vol. 66, no. 6, pp. 4967–4983, Jun. 2017.
- [20] J. S. Yeom, H. S. Jang, K. S. Ko, and B. C. Jung, "BER performance of uplink NOMA with joint maximum-likelihood detector," *IEEE Trans. Veh. Technol.*, vol. 68, no. 10, pp. 10295–10300, Oct. 2019.
- [21] M. K. Simon and M.-S. Alouini, *Digital Communication Over Fading Channels*, vol. 95. Hoboken, NJ, USA: Wiley, 2005.
- [22] A. Goldsmith, *Wireless Communications*. Cambridge, U.K.: Cambridge Univ. Press, 2005.
- [23] I. S. Gradshteyn and I. M. Ryzhik, *Table of Integrals, Series, and Products*. New York, NY, USA: Academic, 2014.